Novel Multilayered Ti/TiN Diffusion Barrier for Al Metallization

WEN-FA WU,[1,4] KOU-CHIANG TSAI,[1,2] CHUEN-GUANG CHAO,[2] JEN-CHUNG CHEN,[2] and KENG-LIANG OU [3]

1.—National Nano Device Laboratories, Hsinchu 300, Taiwan, Republic of China. 2.—Department of Materials Science and Engineering, National Chiao Tung University, Hsinchu 300, Taiwan, Republic of China. 3.—Graduate Institute of Oral Sciences, Taipei Medical University, Taipei, Taiwan, Republic of China. 4.—E-mail: wfwu@mail.ndl.org.tw

A novel, multilayered Ti/TiN diffusion barrier is proposed and successfully applied for Al metallization. The multilayered Ti/TiN structure is effective in enhancing the barrier properties since the very thin Ti layer inserted into titanium nitride (TiN) barrier can cause disruption of the TiN columnar growth and reduction of open grain boundaries resulting in retarded interdiffusion between metal and silicon. Multilayered Ti/TiN films are deposited sequentially by sputtering without breaking vacuum. It is found that TiN grain boundaries are discontinuous when a Ti layer is inserted into TiN. Multilayered Ti/TiN has a better barrier performance than single-layer TiN in Al metallization. However, the barrier performance is related to the number and thickness of the inserted Ti layers, because increasing titanium will enhance chemical reactions between Al and barrier layers, and produce more titanium-aluminum compounds. The total thickness of introduced Ti layers should be reduced to improve barrier performance.

Key words: Diffusion barrier, titanium nitride, multilayer, aluminum

INTRODUCTION

An interconnection system with a barrier metal layer is indispensable in submicron ultra-large-scale integrated devices to realize high reliability such as resistance against electromigration, hillocks, stress-induced voids, and Si precipitation at silicon/metal interfaces.[1,2] Many diffusion-barrier materials have been studied for the Al-Si contact system. Reactively sputtered titanium nitride (TiN) film has been widely used as a diffusion barrier layer between the aluminum and the silicon substrate due to its high thermal and chemical stability, low electrical resistivity, and excellent mechanical properties.[3–5] The stoichiometric TiN has a NaCl-type face-centered cubic structure with a lattice constant of 4.24 Å. The phase is stable over a broad composition range concerning the nitrogen concentration.[6] In general, resistivity of TiN film depends on the deposition conditions, and minimum resistivity has been found at a composition corresponding to stoichiometric TiN.[7]

(Received November 2, 2004; accepted February 28, 2005)

Devices with Al interconnects require some thermal processes to improve interface property and achieve low contact resistance. It is reported that sputtered TiN film has a columnar grain structure with both inter- and intracolumnar voids.[8–10] The dominant failure of TiN diffusion barrier is attributed to diffusion via fast diffusion paths in columnar grains.[11,12] When TiN film is used as the diffusion barrier in Al metallization, Al and Si interdiffuse through the grain boundaries of the TiN film during annealing at elevated temperature, resulting in degradation of the electrical characteristics and device failure. Barrier performance of TiN layer can be improved by in-situ plasma treatment and stuffing grain boundaries with a thin Al interlayer.[1,13,14]

The purpose of this work is to demonstrate a novel, multilayered Ti/TiN diffusion barrier for Al metallization. Al-contacted systems with high thermal stability are obtained. It is found that fast diffusion paths in columnar TiN grains are destroyed when a thin Ti layer is inserted into TiN. Additionally, effects of number, thickness, and distribution of inserted Ti layer on barrier properties of multilayered Ti/TiN films are investigated.

EXPERIMENTAL PROCEDURE

The structure of the Al/barrier/Ti/n^+-p junction diode was used to investigate the barrier capabilities of multilayered Ti/TiN films in this work. The starting materials were p-type (100)-oriented silicon wafers with resistivity of 15–25 Ω cm. The wafers were administered a local oxidation of silicon process to define active regions after RCA cleaning. The n^+-p junctions were formed by As^+ implantation at 60 keV with a dose of 5×10^{15} cm^{-2} and subsequent rapid thermal annealing in N_2 ambient at 1,050°C for 30 sec. The Al alloy (Al-Si-Cu), Ti, and TiN films were deposited by sputtering in a multichamber cluster system without breaking vacuum. The wafers were dipped in a dilute HF solution (HF: H_2O = 1:50) to remove native oxide prior to loading into the system. The Ti layer, 40-nm thick, was deposited onto the Si substrate first and employed as a conventional contact metal layer to improve contact property. Reactively sputtered TiN film, 100-nm thick, was used as the standard (STD) barrier layer. Multilayered Ti/TiN films were prepared by inserting thin Ti layers into the TiN barrier. Various multilayered Ti/TiN films, as summarized in Table I, were employed to investigate the effects of number, thickness, and distribution of the inserted Ti layer on barrier properties. The total thickness of multilayered Ti/TiN barrier layer was 100 nm. Al-Si-Cu film was deposited on top of the barrier layer at 15 kW and 200°C. All samples were alloyed in forming gas ambient at 400°C for 30 min to improve contact properties. The samples were further subjected to a cumulative furnace annealing in forming gas ambient at 500°C for 30 min to investigate thermal stability and barrier performance.

The microstructure and grain size of the film were examined using transmission electron microscopy (TEM). Structure and crystalline orientation of the as-deposited and annealed samples were analyzed by an x-ray diffractometer with Cu K_α radiation operated at 50 kV and 250 mA. Surface roughness and morphology of the film were observed using a Digital Instruments Nanoscope II model atomic force microscope (Vecco, Cleveland, OH) with a 0.5 Hz scanning speed in air ambient. The surface morphology was studied with a field emission scanning electron microscope. Compositional depth profiles analyzed by secondary ion mass spectrometry (SIMS) were used to investigate the Al diffusion after annealing. A four-point probe system was employed to measure sheet resistance. Contact resistance was analyzed using the four-terminal Kelvin structure. Leakage currents of diodes were measured at a reverse bias of 5V by a HP 4156 semiconductor parameter analyzer (Hewlett-Packard, Palo Alto, CA).

RESULTS AND DISCUSSION

Figure 1 shows cross-sectional TEM micrographs of the typical TiN and multilayered Ti/TiN films. Typical columnar grain structure is observed for conventionally sputtered TiN barrier layer, as shown in Fig. 1a. A sawtooth profile is exhibited in a projected two-dimensional view as is expected for films with

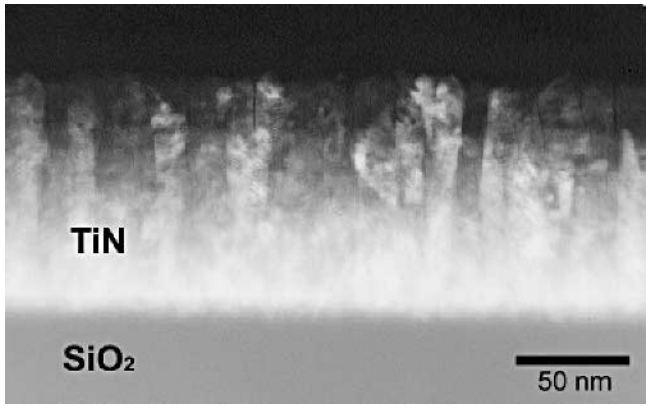

a

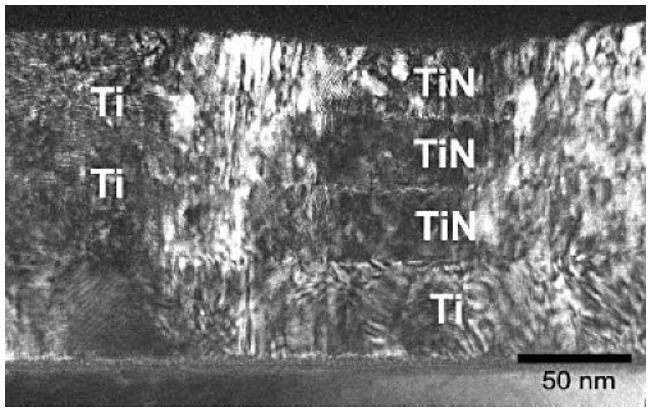

b

Fig. 1. Cross-sectional TEM images of (a) typical TiN film on the SiO_2/Si substrate and (b) multilayered Ti/TiN (TiN-3) film on the Ti/Si substrate. The thickness of typical TiN and TiN-3 barriers is 100 nm.

Table I. Contact Systems with Various Multilayered Ti/TiN Barriers Used in the Study

Barrier Type	Thickness of Ti/TiN (nm)	Thickness of Ti Contact Layer (nm)
TiN-1	TiN (100)	40
TiN-2	TiN (47.5)/Ti (5)/TiN (47.5)	40
TiN-3	TiN (30)/Ti (5)/TiN (30)/Ti (5)/TiN (30)	40
TiN-4	TiN (21.3)/Ti (5)/TiN (21.2)/Ti (5)/TiN (21.3)/Ti (5)/TiN (21.2)	40
TiN-5	TiN (45)/Ti (10)/TiN (45)	40
TiN-6	TiN (42.5)/Ti (15)/TiN (42.5)	40
TiN-7	TiN (25)/Ti (5)/TiN (75)	40
TiN-8	TiN (75)/Ti (5)/TiN (25)	40

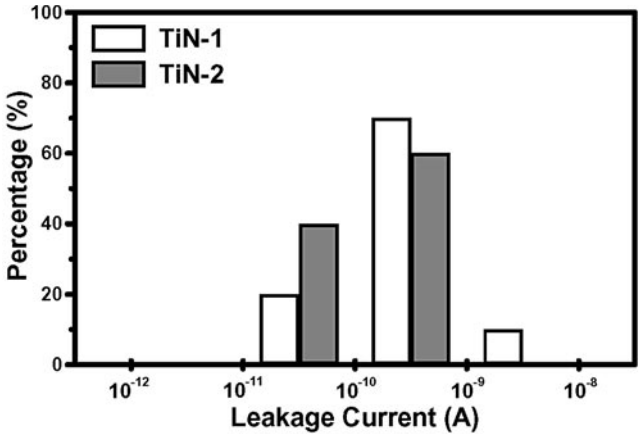

Fig. 2. Histograms showing statistical distributions of reversed-biased leakage currents of Al/TiN (100 nm)/Ti/Si and Al/TiN (47.5 nm)/Ti (5 nm)/TiN (47.5 nm)/Ti/Si junction diodes after annealing at 500°C for 30 min.

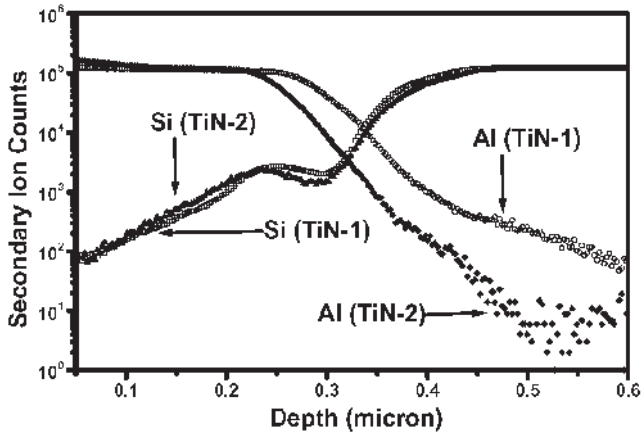

Fig. 3. The SIMS depth profiles of Al/TiN-1/Si and Al/TiN-2/Si contact systems after annealing at 500°C for 30 min.

voided grain boundaries for which growth proceeds in a three-dimensional mode. The trace of the surface facets is along the [022] direction that is consistent with the facets being {111} planes. Discontinuous columnar grains are successfully formed as a very thin Ti layer is inserted into the TiN barrier, as shown in Fig. 1b. The thickness of the Ti layer inserted into TiN to form multilayered Ti/TiN films is 5 nm. The very thin Ti interlayer will cause disruption of the TiN columnar growth. Figure 2 shows the statistical distributions of leakage currents of Al/barrier/Ti/Si junction diodes. Al-contacted junction diodes with multilayered Ti/TiN (TiN-2) barriers exhibit lower leakage currents than those with STD TiN (TiN-1) barriers after cumulative annealing at 500°C for 30 min, indicating that multilayered Ti/TiN structure has successfully impeded the interdiffusion of Al and Si. The SIMS process is further employed to investigate the barrier capability of multilayered Ti/TiN film against diffusion. Figure 3 plots SIMS depth profiles of Al and Si for the Al/barrier/Si system after annealing at 500°C for 30 min. It is also found that Al is less diffused in the multilayered Ti/TiN sample than that in the STD sample.

Figure 4 schematically shows the possible brief reactions of the Al/Ti/Si, Al/TiN/Ti/Si, and Al/TiN/

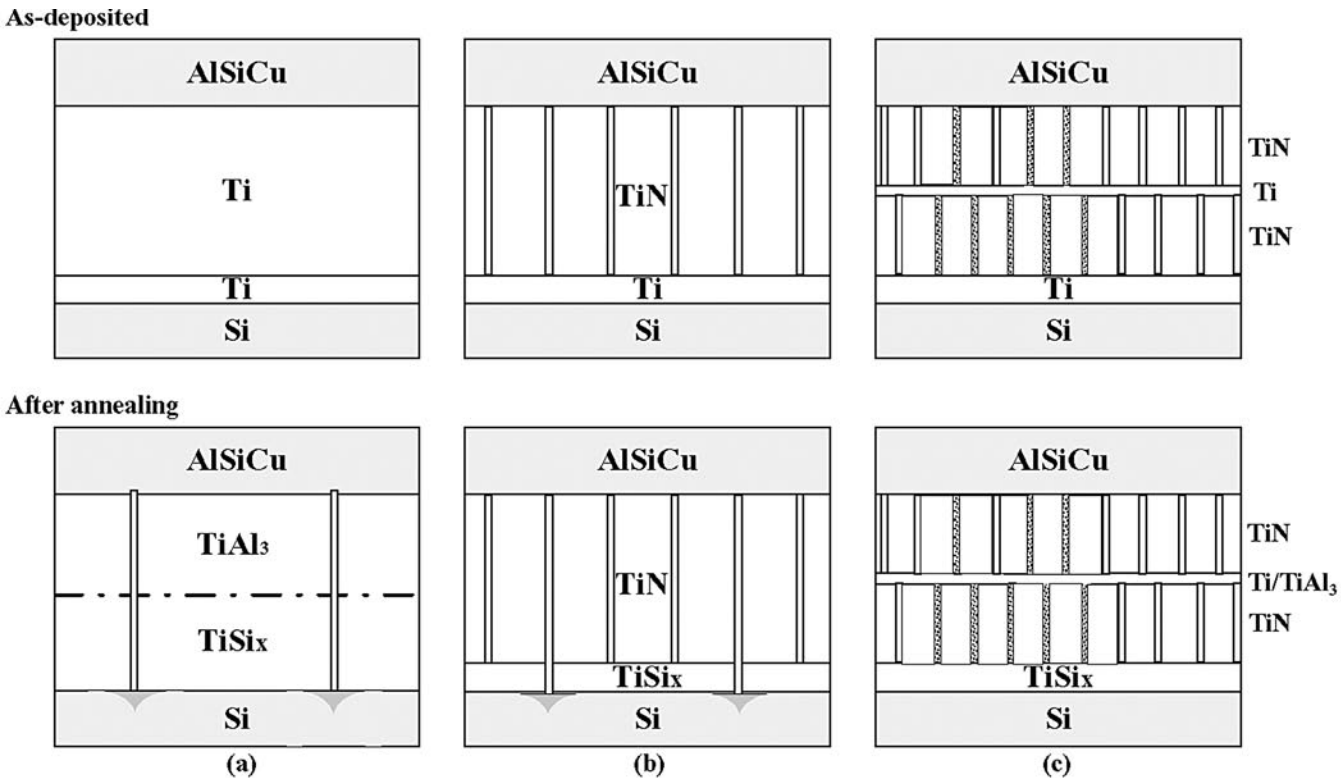

Fig. 4. Schematic illustrations of the possible brief reactions of the Al/Ti/Si, Al/TiN/Ti/Si, and Al/TiN/Ti/TiN/Ti/Si contact systems before and after high-temperature annealing.

Ti/TiN/Ti/Si contact systems before and after high-temperature annealing. It is reported that the Ti layer between Al and Si behaves as a sacrificial barrier because it reacts with Al to form $TiAl_3$ compounds at temperatures above 400°C. The Ti is a good diffusion barrier as long as the Ti is not completely consumed. Once the Ti has completely reacted to form $TiAl_3$, its diffusion barrier properties are lost. It is expected that $TiAl_3$, $TiSi_x$, and Al spiking will be formed for the Al/Ti/Si contact system after high-temperature annealing, as shown in Fig. 4a. The TiN is also an attractive barrier material because it is chemically and thermodynamically stable and behaves as a passive barrier. However, it is typical to form TiN films with columnar grains, as mentioned previously. It is expected that Al and Si would interdiffuse through the grain boundaries of the typical columnar TiN barrier during annealing, which results in spiking in the Si substrate, as shown in Fig. 4b. Discontinuous columnar grains are formed for the multilayered Ti/TiN barrier, as indicated in the TEM image in Fig. 1b. The diffusion has been relatively reduced, as shown in Fig. 3, because the thin Ti interlayer has successfully resulted in disruption of the TiN columnar growth and reduced open grain boundaries of TiN film. Furthermore, the inserting Ti interlayer creates a binding spot for Al. Short-circuit diffusion paths through the TiN would be plugged by the Ti or Ti-Al compound. In order to further explore effects of very thin Ti interlayer on barrier capabilities and thermal stabilities, multilayered Ti/TiN films with various numbers, thicknesses, and distributions of Ti interlayer were prepared and used in this work.

Effects of the Number of Ti Interlayer

Figure 5 shows the x-ray diffraction (XRD) spectra of as-deposited STD TiN and multilayered Ti/TiN barriers with various numbers of the Ti interlayer on Ti/Si substrates. All the XRD patterns show three peaks of TiN (111), Ti (10–11), and Ti (0002). Ti (10–11) and Ti (0002) peaks are believed to result from 40-nm Ti contact layer on the Si substrate because it is much thicker than inserting Ti interlayer. The high (0002) orientation of underlying Ti layer will enhance the development of TiN (111) preferred orientation since they have similar atomic arrangement patterns. The (111) planes of TiN are built of alternate Ti and N layers and are the most closely packed planes.[15] The relative intensity of the TiN (111) peak in the TiN-2 sample is lower and the peak shape becomes broader than that in the TiN-1 (STD TiN) sample, indicating that grain size decreases in the TiN-2 sample. Moreover, the relative intensity of the TiN (111) peak in the TiN-3 sample is much lower and the peak shape becomes broader than that in the TiN-2 sample. That is, the more the Ti-inserting layer, the lower the relative intensity of TiN (111) and the broader the peak shape. It is reported that the first 10-nm or 20-nm TiN films grow in an amorphous-like or nanograined

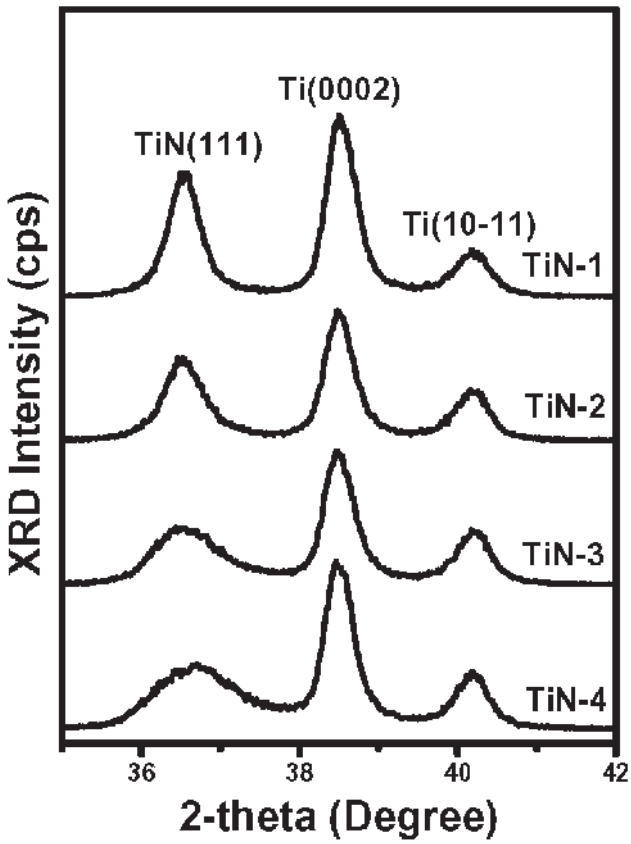

Fig. 5. XRD spectra of as-deposited TiN-based barriers on Ti/Si substrates.

structure followed by columnar grain growth. The columns in the TiN film increase in size with an increase in distance from the film/substrate interface.[16] The nanocrystalline barrier is more effective than the polycrystalline barrier since the nanocrystalline film can slow interdiffusion.[13,17–21] The nanocrystal TiN grains in the multilayered Ti/TiN barrier will enhance the effectiveness of the barrier. Furthermore, the Ti interlayer will turn into an aluminide, causing a step change in Al composition, and thus a lower concentration gradient for Al below the Ti layer. The step change will reduce the gradient of Al diffusion flux. The diffusion barrier performance of TiN film is significantly improved by inserting a thin Ti interlayer into TiN, as shown in Figs. 2 and 3.

Figure 6 shows the variation percentage in sheet resistance of the Al/barrier/Ti/Si sample as a function of the annealing temperature for various multilayered Ti/TiN barrier layers. The samples are subjected to a cumulative furnace annealing in forming gas environment from 400°C to 550°C for 30 min. Sheet resistance increases with increasing annealing temperature. The increase in sheet resistance is attributed to formation of the compounds. The increasing rate in sheet resistance of the STD-TiN (TiN-1) sample is higher than those in multilayered Ti/TiN (TiN-2, TiN-3, and TiN-4) samples, as indicated in Fig. 6. Low increasing rate for multilayered Ti/TiN

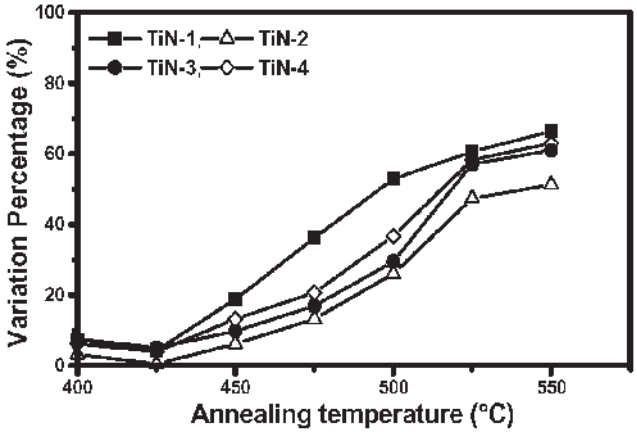

Fig. 6. Variation percentage in sheet resistance of Al/barrier/Ti/Si contact system as a function of annealing temperature.

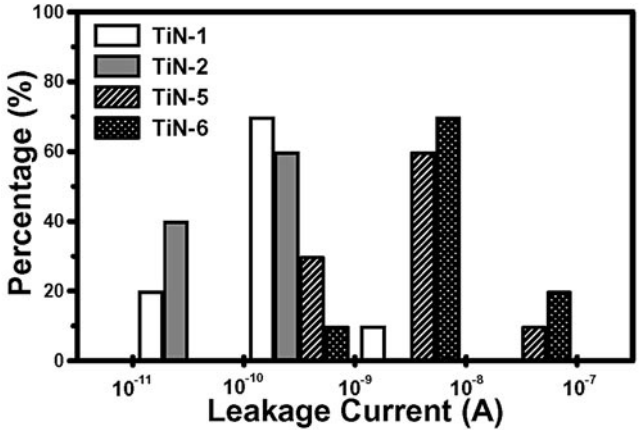

Fig. 7. Histograms showing statistical distributions of reversed-biased leakage currents of Al/barrier/Ti/Si junction diodes after annealing at 500°C for 30 min.

samples is believed to result from discontinuous columnar grains in multilayered Ti/TiN films, which alleviate the interdiffusion and formation of the compound. It is also seen in Fig. 6 that the increasing rate in sheet resistance of the TiN-3 sample is higher than that in the TiN-2 sample, and the increasing rate in sheet resistance of the TiN-4 sample is higher than that in the TiN-3 sample. That is, variation percentage in sheet resistance increases with increasing number of Ti interlayer. X-ray diffraction is employed to analyze annealed Al/barrier/Ti/Si samples to more distinctly display the differences among barrier layers. It is found that the relative intensity of the $TiAl_3$ phase increases with increasing Ti interlayer. As mentioned previously, the Ti layer between Al and Si behaves as a sacrificial barrier because Al and Ti start to react with each other at 400°C and above. The limited efficiency is probably caused by the fact that increasing Ti interlayer reduces total effective thickness of TiN in the multilayered Ti/TiN barrier. Barrier performance is determined by a competition among the disruption effect of columnar growth, gradient of Al diffusion flux, and total effective thickness of TiN. A thin Ti interlayer will result in discontinuity or shift in columnar TiN grain and create a binding spot for Al, thus alleviating interdiffusion and improving barrier performance. However, more Ti interlayers will reduce the total effective thickness of TiN, causing barrier performance to be degraded.

Effects of the Thickness of Ti Interlayer

Effects of thickness of the inserting Ti interlayer on the barrier properties of multilayered Ti/TiN films are further investigated. Figure 7 shows the statistical distributions of reverse-biased leakage currents of the diodes with the TiN-1, TiN-2, TiN-5, and TiN-6 barriers. The distributions of reverse-biased leakage currents are measured at a reverse-biased voltage of 5 V after cumulative annealing at 400°C and 500°C for 30 min. Diodes with Al/barrier/Ti/Si exhibit low leakage currents of the order of 10^{-11}–10^{-8} amperes after cumulative annealing at 400°C and 500°C for 30 min. The diodes with TiN-2 barriers show lower leakage currents than those with STD TiN (TiN-1) barriers, indicating that multilayered Ti/TiN structure has successfully impeded the interdiffusion of Al and Si. However, barrier performance is degraded as the thickness of inserting Ti interlayer increases. The diodes with TiN-5 and TiN-6 barriers show higher leakage currents than those with TiN-1 (STD TiN) and TiN-2 barriers. It is felt that increasing the thickness of the Ti interlayer reduces the total effective thickness of TiN in multilayered Ti/TiN barrier since the total thickness of the TiN-based barrier layer is 100 nm. The multilayered Ti/TiN structure is effective in enhancing the barrier performance and retarding Al/Si interdiffusion, but the thick inserting Ti interlayer in multilayered Ti/TiN barrier is not suggested due to resulting degradation in barrier performance.

Figure 8 presents the contact resistance (Rc) of Al/barrier/Ti/Si contact systems, which include multilayered Ti/TiN barriers with various thicknesses of inserting Ti interlayer. It can be seen that the contact resistance in the TiN-2 contact system is lower than that in the TiN-1 (STD TiN) contact system, and the contact resistance of the Al/barrier/Ti/Si contact system increases as the thickness of the Ti interlayer increases. High contact resistance is found after

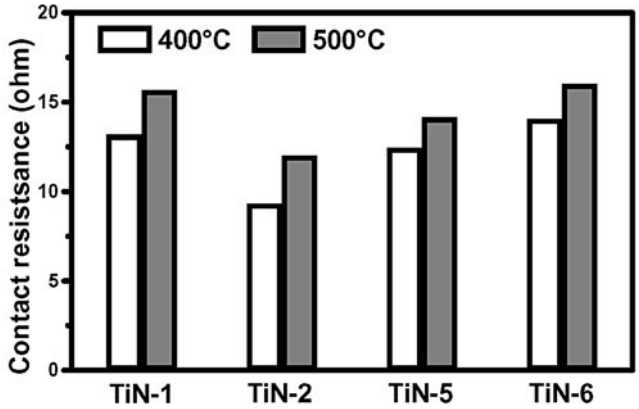

Fig. 8. Contact resistance of Al/barrier/Ti/Si system as a function of thickness of inserting Ti interlayer.

annealing at 500°C because high-temperature annealing will enhance interdiffusion of Al and Si via microscopic defects (i.e., grain boundaries) and formation of the compounds. Low contact resistance in the TiN-2 contact system is attributed to the fact that the additional Ti interlayer has successfully alleviated the interdiffusion of Al and Si. It is important to note that the formation of $TiAl_3$ is more likely to occur in the Al-Ti system than in the Al-TiN system after thermal processing, since thermal stability between Al and Ti layers is lower than that between Al and TiN layers.[22–24] Increased thickness of the inserting Ti interlayer will enhance the formation of $TiAl_3$ compounds, resulting in increased contact resistance.

Effects of the Distribution of Ti Interlayer

Figure 9 shows the statistical distributions of reverse-biased leakage currents of the diodes with TiN-1, TiN-2, TiN-7, and TiN-8 barriers. TiN-2, TiN-7, and TiN-8 barriers have different inserting positions of Ti interlayers in TiN, as summarized in Table I, to explore effects of distribution of inserting Ti interlayer on barrier properties of multilayered Ti/TiN barriers. Superiority of multilayered Ti/TiN as a barrier can be gauged from the leakage current of the diode. Low leakage currents are obtained for multilayered Ti/TiN films compared to the TiN-1 (STD-TiN) sample. Reduction in leakage current of the TiN-7 sample is apparent. Though the detailed mechanisms need to be further investigated, the gradient of Al diffusion flux is believed to be one of the key factors on TiN barrier performance. As mentioned previously, all short-circuit diffusion paths through the TiN would be plugged by the Ti or Ti-Al compounds. If there is a fixed Al concentration on the substrate side of the Ti interlayer, it would be expected that pulling the Ti barrier further away from the Ti contact metal would reduce Al diffusion flux by reducing the gradient. Thin TiN film (25 nm) on the inserting Ti interlayer in the TiN-7 sample leads to better barrier capability due to the reduction of Al diffusion flux.

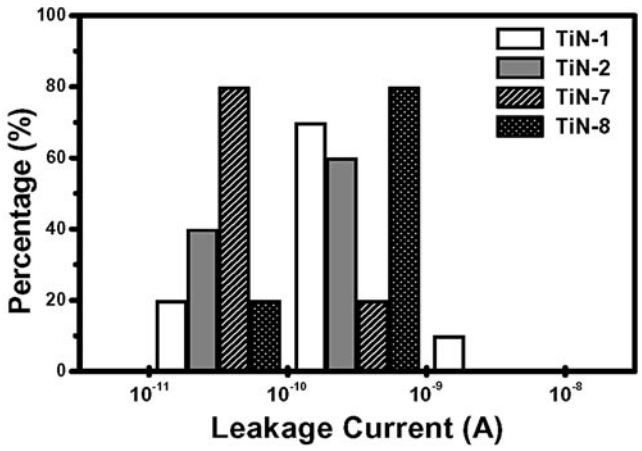

Fig. 9. Histograms showing statistical distributions of reversed-biased leakage currents of Al/barrier/Ti/Si junction diodes after annealing at 500°C for 30 min.

CONCLUSIONS

A novel method to improve TiN-based diffusion barriers using multilayered Ti/TiN structure has been proposed. Multilayered Ti/TiN barriers can alleviate interdiffusion via fast diffusion paths in columnar TiN barriers, because the thin Ti interlayer results in disruption or shift in TiN columnar grains and creates a binding spot for Al. Less interdiffusion is observed in multilayered Ti/TiN barriers from SIMS analyses. The sheet resistance of the Al/TiN/Ti/TiN/Ti/Si contact system is relatively stable compared to the Al/TiN/Ti/Si (STD) contact system. The Al/barrier/Ti/Si junction diodes with multilayered Ti/TiN barriers show relatively low leakage currents compared to those with STD TiN barriers. However, an increase in the number and thickness of the inserting Ti interlayer will reduce efficiency of the TiN-based barrier because Ti is a sacrificial barrier. More titanium layers or increased thickness in the multilayered Ti/TiN film enhances the chemical reactions between Ti and Al. This reduces the total effective thickness of TiN, causing a degradation of barrier performance. As the thickness of the inserting Ti interlayer in TiN increases from 5 nm to 15 nm, degradation of the multilayered Ti/TiN barrier and enhanced formation of $TiAl_3$ are found. The total effective thickness of the inserting Ti interlayer in TiN should be reduced to improve barrier performance. Barrier performance of the multilayered Ti/TiN barrier is also affected by the distribution of the inserting Ti interlayer in TiN. Thin TiN film on the inserting Ti interlayer shows better barrier performance against Al diffusion due to reduced Al diffusion flux.

ACKNOWLEDGEMENTS

This work was financially supported by the National Science Council of the Republic of China (Contract No. NSC 93-2215-E-492-005) and supported, in part, by the Ministry of Economic Affairs of the Republic of China (Contract No. 91-EC-17-A-08-S1-0003). Technical support from the National Nano Device Laboratories is greatly acknowledged.

REFERENCES

1. V. Fortin, S.C. Gujrathi, G. Gagnon, R. Gauvin, J.F. Currie, L. Ouellet, and Y. Tremblay, *J. Vac. Sci. Technol. B* 17, 423 (1999).
2. H. Xiao, *Introduction to Semiconductor Manufacturing Technology* (Upper Saddle River, NJ: Prentice-Hall Inc., 2001), pp. 452–457.
3. C.Y. Ting and M. Wittmer, *Thin Solid Films* 96, 327 (1982).
4. M. Wittmer, *Appl. Phys. Lett.* 37, 540 (1980).
5. C.Y. Ting, *J. Vac. Sci. Technol*. 21, 14 (1982).
6. B. Pécz, N. Frangis, S. Logothetidis, I. Alexandrou, P.B. Barna, and J. Stoemenos, *Thin Solid Films* 268, 57 (1995).
7. B.O. Johansson, J.E. Sundgren, J.E. Greene, A. Rockett, and S.A. Barnett, *J. Vac. Sci. Technol. A* 3, 303 (1985).
8. S.K. Rha, W.J. Lee, S.Y. Lee, Y.S. Hwang, Y.J. Lee, D.I. Kim, D.W. Kim, S.S. Chun, and C.O. Park, *Thin Solid Films* 320, 134 (1998).

9. J.E. Greene, J.E. Sundgren, L. Hultman, I. Petrov, and D.B. Bergstrom, *Appl. Phys. Lett.* 67, 2928 (1995).
10. L. Hultman, J.E. Sundgren, J.E. Greene, D.B. Bergstrom, and I. Petrov, *J. Appl. Phys.* 78, 5395 (1995).
11. J.S. Chun, P. Desjardins, C. Lavoie, I. Petrov, C. Cabral, Jr., and J.E. Greene, *J. Vac. Sci. Technol. A* 19, 2207 (2001).
12. K.Y. Ahn, M. Wittmer, and C.Y. Ting, *Thin Solid Films* 107, 45 (1983).
13. W.F. Wu, K.L. Ou, C.P. Chou, and J.L. Hsu, *Electrochem. Solid-State Lett.* 6, G27 (2003).
14. K.T. Nam, A. Datta, S.H. Kim, and K.B. Kim, *Appl. Phys. Lett.* 79, 2549 (2001).
15. W.F. Wu, C.C. Lin, C.C. Huang, H.C. Lin, T.C. Chang, R.P. Yang, and T.Y. Huang, *Electrochem. Solid-State Lett.* 2, 342 (1999).
16. N. Kumar, J.T. McGinn, K. Pourrezaei, B. Lee, and E.C. Douglas, *J. Vac. Sci. Technol. A* 6, 1602 (1988).
17. D.J. Kim, Y.T. Kim, and J.W. Park, *J. Appl. Phys.* 82, 4847 (1997).
18. K.L. Ou, W.F. Wu, C.P. Chou, S.Y. Chiou, and C.C. Wu, *J. Vac. Sci. Technol. B* 20, 2154 (2002).
19. W.F. Wu, K.L. Ou, C.P. Chou, and C.C. Wu, *J. Electrochem. Soc.* 150, G83 (2003).
20. K.C. Tsai, W.F. Wu, J.C. Chen, T.J. Pan, and C.G. Chao, *J. Vac. Sci. Technol. B* 22, 993 (2004).
21. K.C. Tsai, W.F. Wu, J.C. Chen, T.J. Pan, and C.G. Chao, *J. Electrochem. Soc.* 152, G83 (2005).
22. J.L. Murray, *Phase Diagrams of Binary Titanium Alloys* (Metals Park, OH: ASM, 1987), pp. 13–25.
23. R. Beyers, R. Sinclair, and M.E. Thomas, *J. Vac. Sci. Technol. B* 2, 781 (1984).
24. M. Caron, G. Gagnon, V. Fortin, J.F. Currie, L. Ouellet, Y. Tremblay, M. Biberger, and R. Reynolds, *J. Appl. Phys.* 79, 4468 (1996).